Non-membranous granular organelle consisting of PCM-1: subcellular distribution and cell-cycle-dependent assembly/disassembly

Akiharu Kubo[1,2] and Shoichiro Tsukita[1,2,*]

[1]Department of Cell Biology, Kyoto University Faculty of Medicine, Yoshida-Konoe, Sakyo-ku, Kyoto 606-8501, Japan
[2]Solution Oriented Research for Science and Technology, Japan Science and Technology Corporation, Yoshida-Konoe, Sakyo-ku, Kyoto 606-8501, Japan
*Author for correspondence (e-mail: htsukita@mfour.med.kyoto-u.ac.jp)

Accepted 19 November 2002
Journal of Cell Science 116, 919-928 © 2003 The Company of Biologists Ltd
doi:10.1242/jcs.00282

Summary

Centriolar satellites were initially identified as electron-dense spherical granules, ~70-100 nm in diameter, localized around the centrosomes. We have previously identified pericentriolar material 1 (PCM-1), with a molecular mass of ~230 kDa, as a component of centriolar satellites. We now show by immunofluorescence microscopy that these granules are not only concentrated around centrioles but also scattered throughout the cytoplasm in various types of mouse cells, leading us tentatively to call them 'PCM-1 granules'. We then found that, when overexpressed, PCM-1 molecules lacking their C-terminal region bound directly with each other through two distinct regions to form large aggregates, which then recruited endogenous PCM-1. These large aggregates as well as endogenous PCM-1 granules appear to be disassembled during mitosis, and re-assembled when the cells entered interphase. These findings suggest that PCM-1 granules are formed by self-aggregation of PCM-1 and that this self-aggregation is regulated in a cell-cycle-dependent manner. Furthermore, we found that PCM-1 granules are distinct from pericentrin-containing granules, and that these two distinct types of granular structures are frequently associated with each other within the cytoplasm. These findings are discussed with special reference to the possible physiological functions of PCM-1 granules.

Key words: Centriolar satellites, PCM-1, Centrosome, Pericentrin, γ-Tubulin

Introduction

Centriolar satellites were initially identified by ultrathin section electron microscopy as electron-dense spherical granules ~70-100 nm in diameter and localized around the centrosomes (Bernhard and de Harven, 1960; de-Thé, 1964; Berns et al., 1977; Rattner, 1992). These granules were also called 'mussules' (Bessis and Breton-Gorius, 1958). Similar non-membranous electron-dense spherical granules, called fibrous granules, were reported to appear in large numbers around replicating centrioles during ciliogenesis in ciliated epithelial cells (Steinman, 1968; Sorokin, 1968; Anderson and Brenner, 1971; Dirksen, 1991). Although the relationship between centriolar satellites and fibrous granules remained unclear, these granules were thought to play some important role in the centriolar function, mainly owing to their intimate spatial relationship to centrioles. However, until recently, the lack of information regarding their molecular components has hampered more direct assessment of their structure and functions at the molecular level.

The molecular components of centrosomes have been identified by several distinct methods (Kimble and Kuriyama, 1992; Bornens and Moudjou, 1999). As one of these methods, autoantibodies detected in patients suffering from autoimmune diseases have often been utilized to identify the centrosomal components (Kimble and Kuriyama, 1992; Rattner et al., 1998). A high-titer serum from a patient with systemic sclerosis and Raynaud's phenomenon was identified that contained autoantibodies that specifically recognized centrosomes when mammalian cells were processed for immunofluorescence microscopy (Osborn et al., 1982; Balczon and West, 1991). This serum mainly detected three bands around 39, 185 and 230 kDa by immunoblotting (Balczon and West, 1991), and then a cDNA encoding the ~230 kDa polypeptide was isolated by screening a cDNA expression library. Immunofluorescence microscopy with a polyclonal antibody specific for this polypeptide revealed that this molecule was concentrated in the centrosomes, and then this molecule was designated as pericentriolar material-1 (PCM-1) (Balczon et al., 1994). However, the detailed localization of PCM-1 in centrosomes remained unclarified.

In the previous study, we attempted to identify the centrosomal components by raising monoclonal antibodies against a crude fraction of isolated pericentriolar material from *Xenopus* egg extracts, and we obtained a monoclonal antibody that specifically recognized *Xenopus* PCM-1 (XPCM-1) (Kubo et al., 1999). Interestingly, immunoelectron microscopy revealed that PCM-1 was not distributed diffusely at the pericentriolar region but localized exclusively on centriolar satellites. Using a green fluorescent protein (GFP) fusion protein with PCM-1, we found that PCM-1-positive centriolar satellites moved along microtubules towards their minus ends (i.e. toward the centrosomes) in live

cells as well as in-vitro-reconstituted asters. These findings for the first time defined centriolar satellites at the molecular level and explained their pericentriolar localization. Furthermore, we found that anti-PCM-1 antibodies specifically labeled fibrous granules in ciliogenetic epithelial cells. These findings suggested that centriolar satellites and fibrous granules are identical novel non-membranous organelles containing PCM-1.

In this study, we further examined PCM-1 for a better understanding of the structure and functions of centriolar satellites/fibrous granules. We first found that PCM-1-positive granules were not necessarily concentrated around centrioles but were scattered throughout the cytoplasm in various types of cells. Therefore, in this study, we tentatively call them 'PCM-1 granules'. Interestingly, a detailed examination in cultured cells revealed that PCM-1 granules disappeared during mitosis and re-appeared when the cells proceeded into the interphase. We found that PCM-1 granules were assembled and disassembled in a cell-cycle-dependent manner by regulating the activity of PCM-1 to self-aggregate. Furthermore, we found that PCM-1 granules were distinct from granules containing pericentrin, and that these two distinct types of granular structures frequently associated with each other within the cytoplasm. We believe that the present data provide an important clue to understand the structure and functions of the PCM-1 granule, a novel non-membranous granular organelle.

Materials and Methods

Antibodies and cells

Rabbit anti-*Xenopus* PCM-1 (XPCM-1) polyclonal antibody (pAb) against amino acids (aa) 1346-2031 of XPCM-1, rabbit anti-mouse PCM-1 (mPCM-1) pAb against aa 1299-2025 of mPCM-1, and rat anti-mouse occludin monoclonal antibody (mAb) were raised and characterized previously (Kubo et al., 1999; Saitou et al., 1997). Mouse anti-mouse pericentrin mAb, rabbit anti-pericentrin pAb (PRB-432C), rabbit anti-GFP pAb and mouse anti-glutathione-*S*-transferase (GST) mAb (B-14) were purchased from BD Biosciences, Babco, Molecular Probes and Santa Cruz Biotechnology, respectively. Mouse anti-γ-tubulin mAb (GTU-88), Cy3-conjugated rabbit anti-γ-tubulin pAb, mouse anti-α-tubulin mAb (DM1A) and FITC-conjugated mouse anti-α-tubulin mAb (FITC-DM1A) were purchased from Sigma.

Xenopus kidney epithelial cell line A6 was grown at 23°C without CO_2 atmosphere in Leivobitz's L-15 medium (GIBCO BRL) supplemented with 10% fetal calf serum (FCS) and antibiotics (100 U ml^{-1} penicillin and 0.2 mg ml^{-1} kanamycin). Mouse L fibroblasts, mouse Eph-4 epithelial cells and mouse CSG epithelial cells were cultured in Dulbecco's modified Eagle's medium supplemented with 10% FCS.

Constructs and transfection

Full-length XPCM-1 (aa 1-2031) was fused with red-shifted GFP (rsGFP) (pQBI25; Quantum Biotechnologies) at its C terminus (GFP-full) as described previously (Kubo et al., 1999). To cut off regions from the GFP-full expression vector to construct a series of deletion mutants of XPCM-1, *Mlu*I sites or *Kpn*I sites were introduced into both ends of the regions by site-directed mutagenesis. The cDNA between *Kpn*I sites or *Mlu*I sites was cut off by *Kpn*I or *Mlu*I digestion followed by self-ligation. All expression vectors were confirmed by sequencing. A6 cells were transfected using LipofectAMINE plus reagent (Invitrogen) and observed 2-3 days after transfection.

Immunofluorescence microscopy

Cells cultured on poly-L-lysine coated coverslips were fixed with methanol for 5 minutes at –20°C, washed in PBS, incubated with 0.12% glycine/PBS for 20 minutes and then processed for immunofluorescence microscopy as described previously (Kubo et al., 1999). In some experiments, A6 cells were incubated in L-15 medium containing 0.4 μM nocodazole for 1 hour, washed twice with fresh medium, incubated in fresh medium for 5 minutes and then fixed with methanol. After washing with PBS, the cells were soaked in 20% FCS in DMEM for 30 minutes and incubated with primary antibodies for 1 hour in a moist chamber. The cells were then washed with PBS and incubated with fluorescently labeled secondary antibodies for 1 hour. Rhodamine-conjugated donkey anti-rabbit IgG antibody (Chemicon), Cy3-conjugated donkey anti-rat IgG antibody (Jackson Laboratory), Alexa Fluor 488-conjugated goat anti-mouse IgG (Molecular Probes) and Cy5-conjugated donkey anti-mouse IgG antibody (Chemicon) were used as secondary antibodies. Samples were then washed with PBS, rinsed in distilled water, mounted in 40% w/w Mowiol (Calbiochem) and then observed using a DeltaVision microscope (Applied Precision) equipped with an Olympus IX70 microscope (Olympus, Tokyo, Japan) and a cooled charge-coupled device (CCD) system. Whole-cell images were obtained with 0.2 μm interval in *z* section, deconvolved and integrated with DeltaVision software (Applied Precision).

Mice were fixed by perfusing 3.7% formaldehyde/PBS from the heart. The intestine, kidney, liver and brain were dissected and rinsed in 3.7% formaldehyde/PBS for 30 minutes. Samples were mounted in Tissue-Tek and frozen using liquid nitrogen. Frozen sections ~12 μm thick were cut on a cryostat, mounted on poly-L-lysine-coated glass coverslips, air-dried and soaked in PBS containing 1% Triton X-100 for 10 minutes. They were then rinsed in PBS and processed for immunofluorescence microscopy as described above.

Granule counting from deconvolved images

Images of whole cells were obtained with 0.2 μm interval in *z* section and deconvolved with DeltaVision software (Applied Precision). To evaluate the immunostaining of granules, a pixel more than three times brighter than the average of the background fluorescent intensity was judged as positive. Using two-dimensional polygon finder of DeltaVision software, we regarded an aggregate consisting more than ten positive pixels (1 pixel = 44.7 nm in diameter) as a single PCM-1 or pericentrin granule, and with three-dimensional (3D) volume builder of DeltaVision software, we reconstituted the 3D images of granules to count the number of granules. In some types of cells, PCM-1 granules were tightly accumulated around centrosomes, so it was difficult to count the number of these granules directly. In such a case, we first measured the average fluorescent intensity of individual PCM-1 granules (FIg) in the cytoplasm, and then calculated the number of PCM-1 granules around centrosomes through dividing the total fluorescent intensity of PCM-1 around centrosomes by FIg.

Yeast two-hybrid

Protein interactions were examined using the MATCHMAKER LexA Two-Hybrid System (Clontech). The cDNA encoding aa 1-484 or aa 745-1273 of XPCM-1 was fused to the DNA-binding domain (DNA-BD) in the pLexA vector and the cDNA encoding aa 1-711 or 745-1273 of XPCM-1 was fused to the activation domain (AD) in the pB42AD vector. DNA-BD and AD constructs were transformed into yeast strain EGY48 (p8op-lacZ). For the positive control, pLexA-53 and pB42AD-T (murine p53 and SV40 large T-antigen were fused to the DNA-BD and AD, respectively) provided by the supplier were transformed. For the negative control, either pLexA-53 or pB42AD-T was transformed instead of XPCM-1 polypeptide fused to DNA-BD or AD, respectively. The activation of reporter genes (*lacZ* and *LEU2*) was tested by replica plating the transformants on SD plate

(with galactose and raffinose to induce the expression of AD fusion proteins, with X-gal to test for *lacZ* expression, with or without leucine to test for *LEU2* expression). SD with glucose was used as a control to verify that the reporter activation was correlated with the induction of AD fusion protein expression.

In vitro binding assay using fusion proteins

The cDNAs encoding aa 745-1271 and aa 1020-1271 of XPCM-1 were fused with 3′-untranslated region of XPCM-1 at their C termini and cloned into baculovirus transfer vectors, pAcGHLT-B and -C (Pharmingen), respectively, to generate GST fusion proteins. Recombinant baculoviruses were generated by co-transfecting the transfer vector with BaculoGold DNA (Pharmingen) into Sf9 cells, and the resulting viruses were amplified by sequential infection into Sf9 cells. The infected cells were harvested, lysed in IP lysis buffer (10 mM Tris, 130 mM NaCl, 1% Triton X-100, 10 mM NaF, 10 mM sodium phosphate, 10 mM sodium pyrophosphate, pH 7.5) on ice for 45 minutes and centrifuged at 45,000 ***g*** for 30 minutes. Pellets were denatured with 4 M urea for 20 minutes at 4°C. After urea was removed by dialysis, the samples were centrifuged at 20,000 ***g*** for 30 minutes. The supernatant containing the renatured recombinant proteins was applied onto glutathione Sepharose 4B columns (Amersham Pharmacia), which were then washed with PBS containing 400 mM NaCl. *Xenopus* interphase egg extracts, prepared as described previously (Shiina et al., 1992), were incubated with the beads for 3 hours at 4°C and the beads were washed with PBS containing 200 mM NaCl and boiled in SDS-PAGE sample buffer. SDS-PAGE and immunoblotting were performed as described previously (Kubo et al., 1999).

Electron microscopy

For ultrathin section electron microscopy, A6 and Sf9 cells or pellets of isolated aggregates were fixed with 2% glutaraldehyde in 0.1 M cacodylate buffer for 2-3 hours at 4°C, washed with 0.1 M cacodylate buffer, followed by incubation with 2% glutaraldehyde in 0.1 M cacodylate buffer containing 0.5% (0.1% for pellets) tannic acid for 1-2 days at 4°C. Samples were then processed for ultrathin section electron microscopy as described previously (Kubo et al., 1999).

For immunoelectron microscopy, A6 cells cultured on glass coverslips were fixed with 0.125% glutaraldehyde in 80PEM buffer (Kubo et al., 1999) containing 2% Triton X-100 for 10 minutes at room temperature, and processed for immunoelectron microscopy as described previously (Kubo et al., 1999). Goat anti-rabbit IgG coupled to 10 nm gold particles (Nycomed Amersham) was used as a secondary antibody. Samples were examined with an electron microscope (JEM 1010; JEOL) at an accelerating voltage of 100 kV.

Observation of GFP fusion proteins in live cells

A6 cells were transiently transfected with various truncated forms of XPCM-1, which were fused with GFP, and cultured for 2 days. These transfectants were observed using a DeltaVision microscope (Applied Precision). Each image was acquired with 1-second exposure of the CCD camera.

Results

Widespread occurrence of PCM-1 positive granules

Using anti-mouse PCM-1 (mPCM-1) pAb, we first examined the distribution of PCM-1 granules in cultured mouse fibroblasts and epithelial cells that were counter-stained with anti-α-tubulin mAb and anti-γ-tubulin mAb. In cultured L fibroblasts, some PCM-1 granules appeared to be concentrated around the centrosomes but the other granules were scattered through the cytoplasm (Fig. 1a). Also, in cultured Eph-4 epithelial cells, PCM-1 granules were gathered around the centrosomes located in the apical region of the cytoplasm and, again, many granules were found in the cytoplasm (Fig. 1b). They showed an intimate spatial relationship with microtubules.

We examined in detail the occurrence and distribution of PCM-1 granules in various types of mouse organs. Their frozen sections were double stained with anti-mPCM-1 pAb and anti-α-tubulin mAb. In all the types of cells we examined, PCM-1 granules were detected, although their number per cell varied significantly depending on the cell types. As previously reported (Kubo et al., 1999), in ciliated epithelial cells in the oviduct and trachea, a large number of PCM-1 granules were accumulated around the basal bodies of cilia (data not shown). Interestingly, even in intestinal and renal epithelial cells, which did not bear cilia, PCM-1 granules were concentrated abundantly in the apical region of the cytoplasm (Fig. 1c,d). In hepatocytes, however, a fairly small number of PCM-1 granules were detected and counter staining with anti-occludin mAb revealed that PCM-1 granules were scattered around the bile canaliculi, where the centrosomes were located (Fig. 1e). In contrast, in nerve cells in the brain, PCM-1 granules were scattered over the cytoplasm showing no significant concentration around the γ-tubulin-positive centrosomes (Fig. 1f).

These findings indicated that PCM-1 granules are novel non-membranous organelles that occur ubiquitously in various types of cells. Furthermore, the immunofluorescence images in Fig. 1a-f raised a simple question to what extent PCM-1 granules are distributed around centrosomes. To answer this question, we quantitatively evaluated the spatial relationship between PCM-1 granules and centrosomes using four distinct types of cultured cells (Fig. 1g). We counted the number of PCM-1 granules inside and outside a 3 μm radius of the γ-tubulin-positive centrioles as described in detail in Materials and Methods. The total number of PCM-1 granules per cell did not appear to be different significantly among cell types (~300-500 granules cell^{-1}) but, as expected from Fig. 1a-f, their spatial relationship with centrosomes varied significantly depending on cell types. For example, in L fibroblasts and CSG epithelial cells, only 13±2% (mean±s.e.m.; n=16) and 14±2% (n=18) of PCM-1 granules occurred around centrosomes, respectively, whereas, in A6 epithelial cells, 64±5% (n=8) was found within a 3 μm radius of centrioles. In this sense, it would be misleading, if PCM-1 granules are called ‘centriolar satellites’.

Domains of PCM-1 responsible for its self-aggregation

Next, we examined how PCM-1 is involved in the formation of PCM-1 granules. As previously reported, when the GFP fusion protein with full-length *Xenopus* PCM-1 (XPCM-1-GFP) was exogenously expressed at a relatively low level in *Xenopus* A6 cells, XPCM-1-GFP was recruited to PCM-1 granules containing endogenous XPCM-1 (data not shown). Then, we constructed GFP fusion proteins with various deletion mutants of XPCM-1 and introduced them into A6 cells. Interestingly, we found that some deletion mutants formed large aggregates within the cytoplasm when

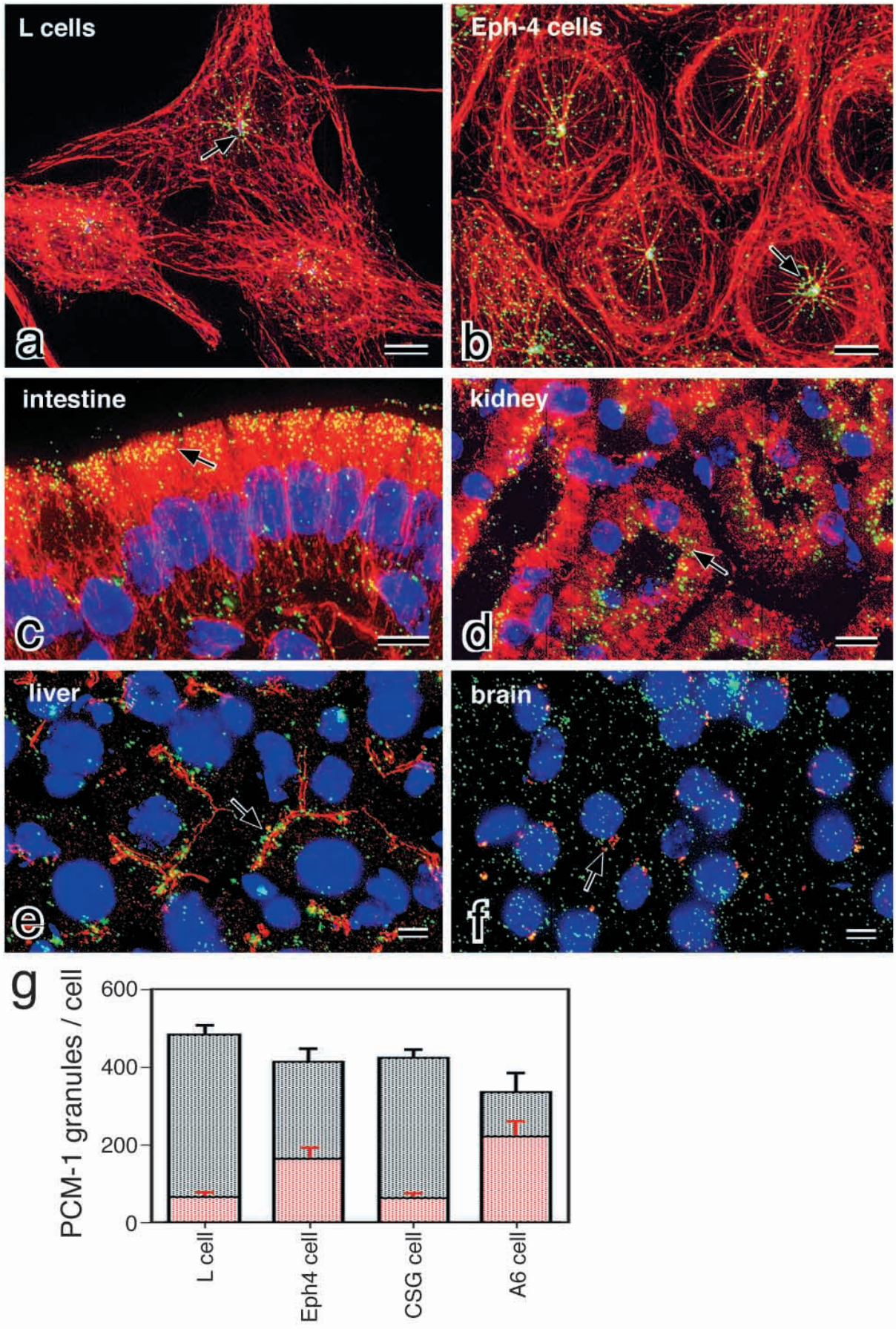
L cells
Eph-4 cells
intestine
kidney
liver
brain
a
b
c
d
e
f
g
PCM-1 granules / cell
600
400
200
0
L cell
Eph4 cell
CSG cell
A6 cell

Fig. 1. Widespread occurrence of PCM-1 granules. Cultured mouse L fibroblasts (a), Eph-4 epithelial cells (b) or frozen sections of mouse intestine (c) or kidney (d) were triple stained with anti-mPCM-1 pAb (green), anti-α-tubulin mAb (red) and anti-γ-tubulin mAb (blue, turned white) (a,b) or anti-mPCM-1 pAb (green), anti-α-tubulin mAb (red) and DAPI (blue) (c,d). In cultured cells (a,b), some PCM-1 granules were gathered around the centrosomes (arrows) but the others were scattered in the cytoplasm. In intestinal and renal epithelial cells (c,d), PCM-1 granules were concentrated abundantly in the apical region of the cytoplasm (arrows). The liver (e) or the brain (f) were triple stained with anti-mPCM-1 pAb (green), anti-occludin mAb (red) and DAPI (blue) (e) or anti-mPCM-1 pAb (green), Cy3-conjugated anti-γ-tubulin pAb (red) and DAPI (blue) (f). In hepatocytes (e), a fairly small number of PCM-1 granules were detected, which were scattered around the occludin-positive bile canaliculi (arrow) where the centrosomes (and minus ends of microtubules) were located. In nerve cells in the brain (f), PCM-1 granules were scattered over the cytoplasm, showing no significant concentration around the γ-tubulin-positive centrosomes (arrow). Bars, 10 μm. (g) To clarify the spatial relationship of PCM-1 granules with centrosomes quantitatively, four distinct types of cultured cells were double stained with anti-mPCM-1 pAb and Cy3-conjugated anti-γ-tubulin pAb, and the number of PCM-1 granules inside (red) and outside (black) a radius of 3 μm of the γ-tubulin-positive centrioles were counted for 16 L cells, 10 Eph4 cells, 18 CSG cells and 8 A6 cells as described in Materials and Methods. Error bars show the s.e.m.

overexpressed; one example of the formation of such aggregates by a XPCM-1 deletion mutant (aa 745-1273) is shown in Fig. 2A. Immunostaining of these cells with anti-XPCM-1 pAb, which recognized endogenous XPCM-1 but not the exogenous XPCM-1 mutant, revealed that not only exogenous XPCM-1 mutant but also endogenous XPCM-1 were incorporated into these aggregates. On ultrathin-section electron microscopy, these large aggregates were observed as homogeneous electron-dense structures lacking delineating membranes (Fig. 2B). These findings suggested that PCM-1 has an ability to self-aggregate to form granular structures.

Fig. 2C summarizes the ability of the formation of large aggregates for various deletion mutants of XPCM-1. Two non-overlapping segments (aa 201-494 and aa 745-1128) formed large aggregates independently when overexpressed, and recruited endogenous XPCM-1 to them. The Coils program (Lupas et al., 1991) predicted multiple short coiled-coil regions within both segments (data not shown). These findings suggested that XPCM-1 molecules interact with each other through at least two independent regions. Furthermore, considering that either full-length XPCM-1 or a truncated XPCM-1 carrying the C-terminal region (aa 487-2031) did not form large aggregates, it was likely that the C-terminal region of XPCM-1 had the ability to suppress the formation of large aggregates.

Then, we examined whether the intermolecular interaction of XPCM-1 is direct or indirect. First, we performed yeast two-hybrid analyses. The cDNA encoding aa 1-484 or aa 745-1273 of XPCM-1 was fused to DNA-BD in the pLexA vector and the cDNA encoding aa 1-711 or aa 745-1273 to AD in the pB42AD vector. DNA-BD and AD constructs were then transformed into yeast. As shown in Fig. 3A, aa 1-484 and aa 745-1273 bound directly to aa 1-711 and aa 745-1273, respectively. Although the possibility has not been theoretically excluded that some yeast protein functions as an intermediate partner in these binding, these findings strongly favored the notion that the intermolecular interaction of XPCM-1 is direct. Next, we overexpressed a GST fusion protein with XPCM-1 fragment (aa 745-1271) in insect Sf9 cells. Electron microscopy revealed that, in Sf9 cells, large aggregates were also formed in the cytoplasm, as observed in A6 cells (Fig. 3Ba). When these cells were lysed with a detergent followed by appropriate centrifugation, these aggregates were partially isolated as pellets (Fig. 3Bb). Interestingly, when these pellets were separated by SDS-PAGE, the GST-XPCM-1 fragment was detected as only one major component (Fig. 3C), indicating that these aggregates were formed through the direct intermolecular binding of XPCM-1 without an intermediate partner. Finally, we constructed a column consisting of the GST-XPCM-1 fragment (aa 745-1271 and aa 1020-1271) to which the whole lysate of *Xenopus* interphase egg extract was applied. The bound proteins were then eluted and immunoblotted with anti-XPCM-1 pAb. As shown in Fig. 3D, endogenous full-length XPCM-1 bound to aa 745-1271 but not to aa 1020-1271. This binding might explain how endogenous PCM-1 is recruited to the large aggregates induced by the overexpression of exogenous truncated PCM-1. These findings led us to speculate that the PCM-1 granules are formed by the self-aggregation of PCM-1.

Cell cycle-dependent assembly and disassembly of PCM-1 granules

PCM-1 was previously reported to concentrate at the centrosomes during interphase but not during the mitotic phase, although PCM-1 granules have not yet been identified at that time (Balczon et al., 1994). Consistently, A6 cells at the interphase were characterized by numerous PCM-1 granules gathering around the centrosomes, whereas, during the mitotic phase, the PCM-1 granules became mostly undetectable (Fig. 4A). This finding suggested that, during mitosis, the self-aggregation of PCM-1 is suppressed to disassemble PCM-1 granules. To evaluate this speculation, the behavior of the large aggregates of GFP fusion proteins with truncated PCM-1 constructs was pursued during mitosis. One example of the aggregates of aa 745-1128 (Fig. 2C) is shown in Fig. 4B. When A6 transfectants proceeded into the mitotic phase with concomitant rounding-up, the aggregates rapidly reduced in size. Furthermore, at the end of mitosis, the aggregates grew again to their original size. These findings indicated that, during the mitotic phase, there is some molecular mechanism that suppresses the self-aggregation of PCM-1, i.e. it facilitates the disassembly of PCM-1 granules.

Relationship between PCM-1 granules and pericentrin granules

PCM-1 was reported to associate with pericentrin (Li et al., 2001), a component of pericentriolar material, which forms a large protein complex with the γ-tubulin ring complex (Dictenberg et al., 1998). Therefore, we next examined the relationship between PCM-1 granules and pericentrin/γ-tubulin. When A6 transfectants bearing large aggregates of a GFP fusion protein with a truncated XPCM-1 (aa 745-1128; Fig. 2C) were double stained with anti-pericentrin pAb and

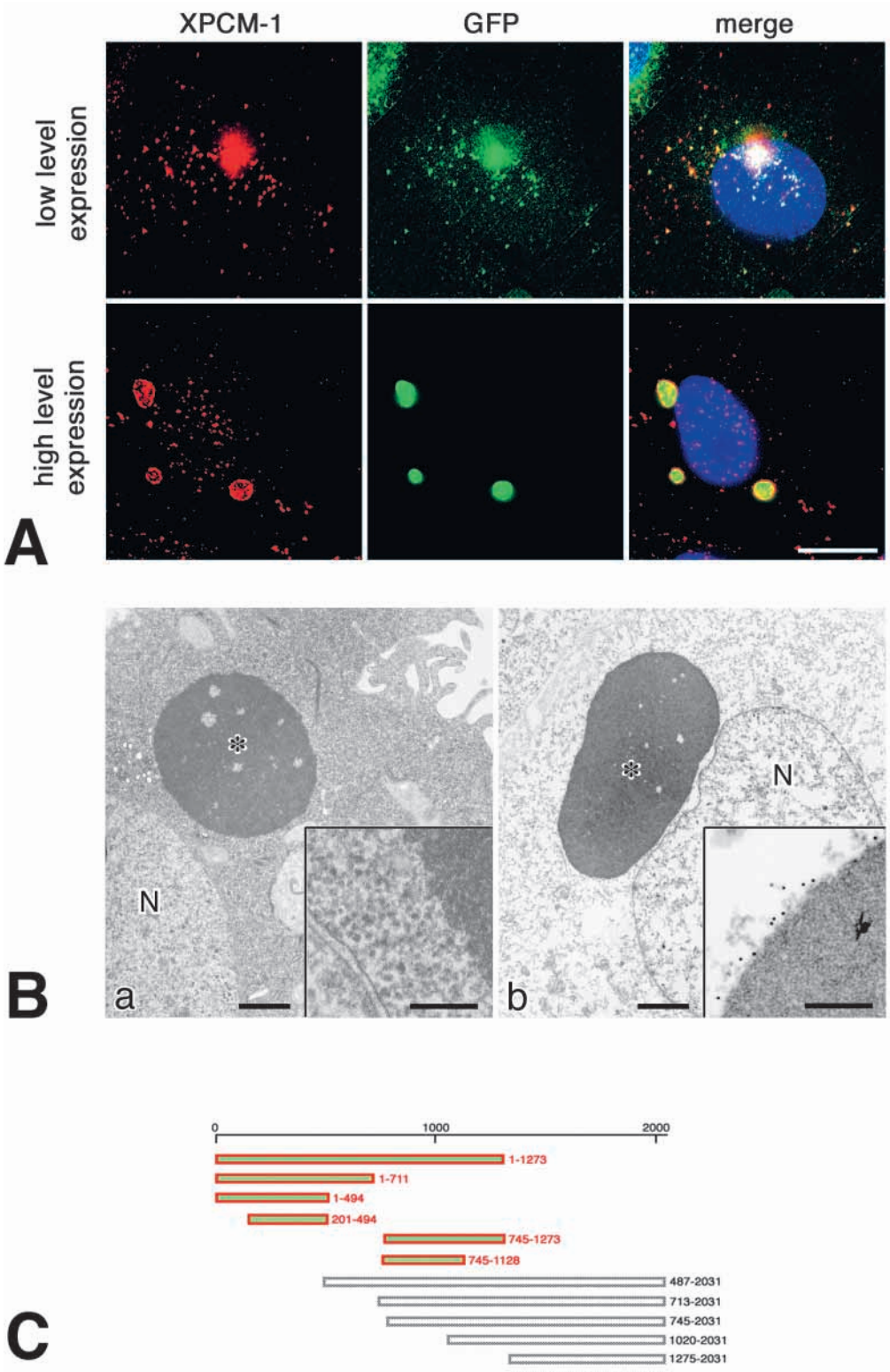

Fig. 2. Formation of large aggregates consisting of PCM-1 deletion mutants. (A) *Xenopus* A6 cells were transfected with cDNA encoding a GFP fusion protein with a truncated XPCM-1 mutant (aa 745-1273; C). Transfectants expressing small or large amounts of the GFP fusion protein were double stained with anti-XPCM-1 pAb (red) and DAPI (blue). This pAb recognized endogenous XPCM-1 but not the exogenously expressed XPCM-1 mutant. Notice that the GFP-positive large aggregates were formed when the exogenous protein was overexpressed, and that these aggregates recruited endogenous XPCM-1. Bar, 10 μm. (B) Ultrathin section electron microscopy. A6 transfectants overexpressing a GFP fusion protein with a truncated XPCM-1 mutant (aa 745-1273) bore large aggregates, homogenous electron-dense structures (asterisk) (a). Notice that the nucleus, but not these granules, were delineated by membranes (inset). Cells were treated with Triton X-100 and labeled with anti-GFP pAb (b). The surface of the large aggregate (asterisk) was specifically labeled with gold particles (inset). N, nucleus. Bars, (a,b) 500 nm; (inset) 200 nm. (C) The ability of the formation of large aggregates for various deletion mutants of XPCM-1. The constructs represented in color, but not those in black and white, formed large aggregates when overexpressed.

anti-γ-tubulin mAb, both pericentrin and γ-tubulin signals were clearly detected from the aggregates (Fig. 5A), suggesting that, in these cells, pericentrin and γ-tubulin were sequestered from centrosomes (i.e. the ability of the centrosomes to nucleate microtubules would be suppressed). To evaluate this speculation, A6 cells with or without the large aggregates of truncated XPCM-1 were incubated in a medium containing 0.4 μM nocodazole for 1 hour to depolymerize microtubules, washed with fresh medium twice, incubated in fresh medium for 5 minutes to repolymerize the microtubules and then processed for immunofluorescence microscopy with anti-α-tubulin mAb. As shown in Fig. 5B, as expected, a large number of microtubules elongated from the centrosomes in A6 cells without large aggregates of truncated XPCM-1, whereas, in

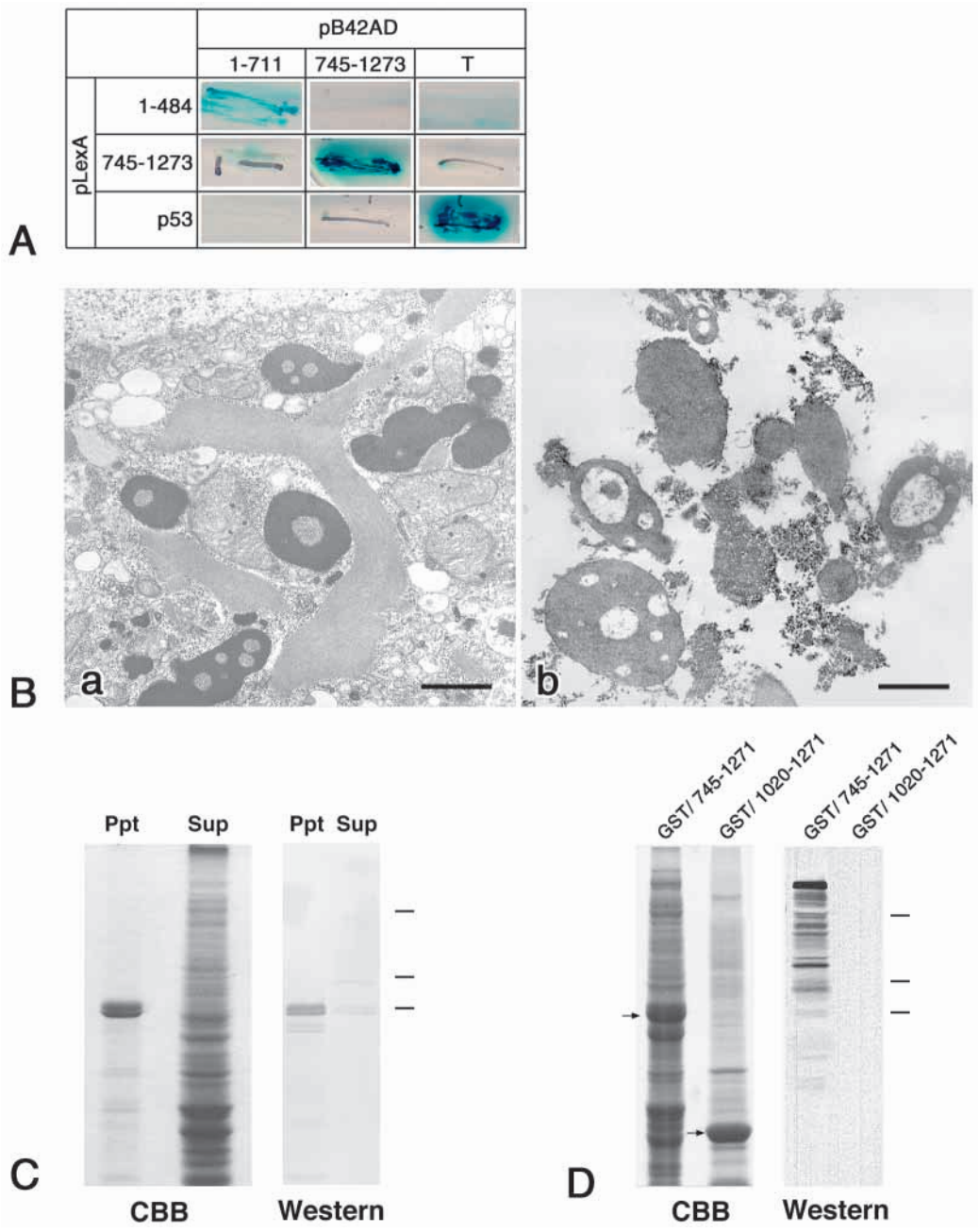

Fig. 3. Self-aggregation of PCM-1. (A) Yeast two-hybrid analyses. The cDNA encoding aa 1-484 or aa 745-1273 of XPCM-1 (p53 as a control) was fused to the DNA-binding domain (DNA-BD) in the pLexA vector and the cDNA encoding aa 1-711 or aa 745-1273 (SV40 large T-antigen as a control) to the activation domain (AD) in the pB42AD vector. DNA-BD and AD constructs were then transformed into yeast. Notice that aa 1-484 and aa 745-1273 bound directly to aa 1-711 and aa 745-1273, respectively. (B) Overexpression of a GST fusion protein with XPCM-1 fragment (aa 745-1271) in insect Sf9 cells. As seen in A6 cells (Fig. 2B), electron-dense large aggregates were formed within the cytoplasm abundantly (a). These Sf9 cells were lysed with 1% Triton X-100 and the lysate was separated by centrifugation. The aggregates were partially isolated as a pellet (b). Bars, 1 μm. (C) Components of the partially isolated aggregates. The pellet (ppt) and supernatant (sup) were separated by SDS-PAGE and stained with Coomassie Brilliant Blue (CBB). The pellet contained only one major band, around 83 kDa (sometimes divided into two bands for an unknown reason), which was identified as the GST-XPCM-1 fragment by immunoblotting with anti-GST mAb (western). Bars represent molecular masses of 203, 116 and 83 kDa from the top. (D) In vitro binding assay. A column consisting of GST fusion proteins with a XPCM-1 fragment (aa 745-1271 and aa 1020-1271) was constructed, to which the whole lysate of *Xenopus* interphase egg extract was applied. Bound proteins were then eluted (CBB) and immunoblotted with anti-XPCM-1 pAb (western). Arrows indicate the GST fusion proteins. Notice that endogenous full-length XPCM-1 bound to aa 745-1271 but not to aa 1020-1271. Bars represent molecular masses of 203, 116 and 83 kDa from the top.

A6 cells bearing large aggregates, only a small number of microtubules were associated with the centrosomes. These findings confirmed the interaction between PCM-1 and pericentrin/γ-tubulin within the cells.

In addition to the pericentriolar localization, pericentrin was also reported to form granular structures scattered in the cytoplasm moving along microtubules (Young et al., 2000) like PCM-1 granules, although these pericentrin granules have not yet been examined in detail by electron microscopy. Therefore, we compared the localization of endogenous PCM-1 with that of endogenous pericentrin in the cytoplasm of CSG cells in detail using sectioning microscopy. As shown in Fig. 5C, PCM-1 granules and pericentrin granules were distributed in the cytoplasm as distinct structures, which were frequently associated with each other in a granule-to-granule manner. Indeed, when we examined the frequency for this association quantitatively in the non-centrosomal region of the cytoplasm using sectioning microscopy, 17±4% (mean±s.e.m.; 54±6/380±45 granules cell^{-1}; n=12) of PCM-1 granules and 48±2% (54±6/113±14 granules cell^{-1}; n=12) of pericentrin granules were associated with each other. These findings suggested that PCM-1 granules and pericentrin granules occur in the cytoplasm independently, and that they dynamically interact with each other.

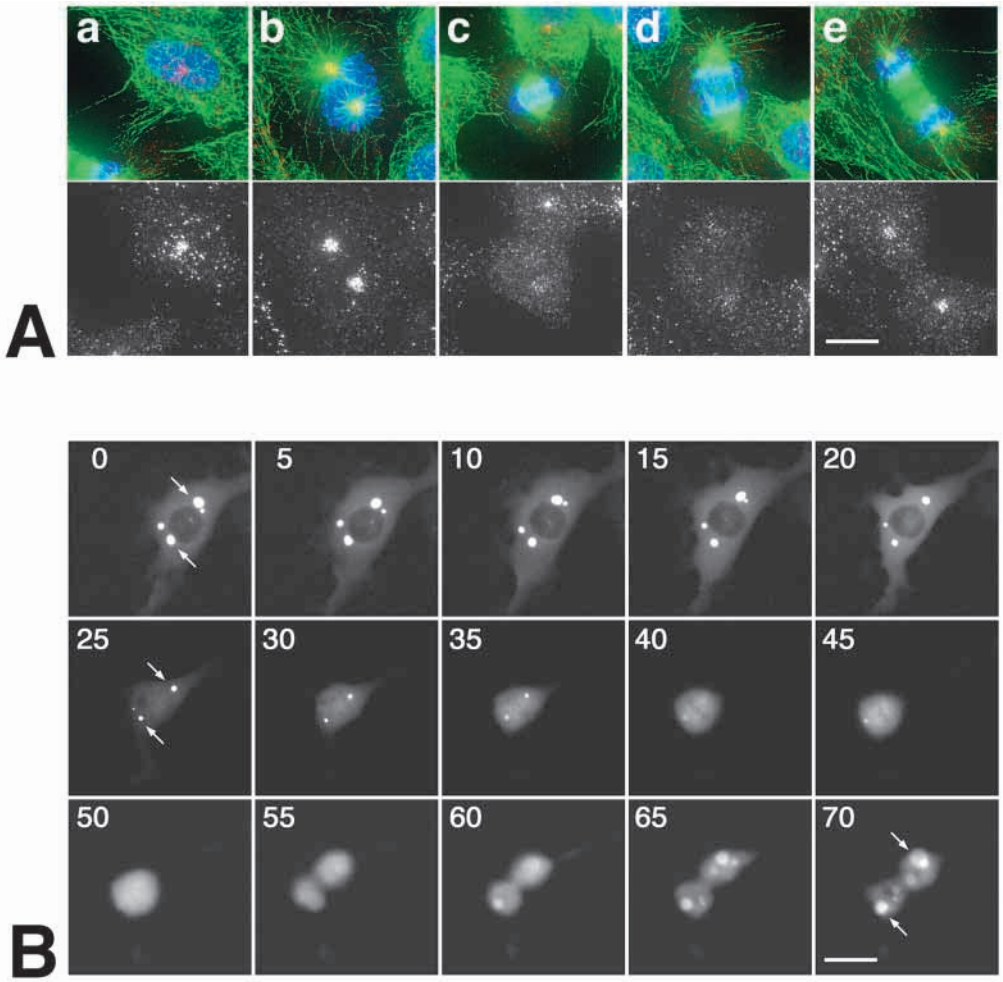

Fig. 4. Cell-cycle-dependent assembly and disassembly of PCM-1 granules and aggregates. (A) A6 cells were triple stained with anti-XPCM-1 pAb (red), FITC-conjugated anti-α-tubulin mAb (green) and DAPI (blue). Lower panels represent only PCM-1 signals. At interphase, PCM-1 granules were scattered around the cytoplasm, showing significant concentration around the centrosomes (a). When cells entered the mitotic phase, PCM-1 granules gathered around two divided centrosomes very intensely (b) and then gradually began to disappear (c,d). At the end of the mitotic phase, PCM-1 granules again gradually appeared around the centrosomes (e). Bar, 10 μm. (B) Time-lapse images of the dynamic behavior of the large aggregates of GFP fusion proteins with a truncated XPCM-1 (aa 745-1128; Fig. 2C) during mitosis. Elapsed time is indicated at the top (in minutes). The large aggregates (arrows) decreased in size when cells entered the mitotic phase with concomitant rounding-up and then recovered to the original size at the interphase. Bar, 10 μm.

Discussion

To date, numerous organelles have been well characterized in terms of their molecular architecture and functions with some exceptions such as centriolar satellites/fibrous granules. Centriolar satellites/fibrous granules were observed more than 40 years ago by electron microscopy (Bessis and Breton-Gorius, 1958; Bernhard and de Harven, 1960; de-Thé, 1964; Steinman, 1968; Sorokin, 1968) but, until we identified PCM-1 as one of its components (Kubo et al., 1999), our knowledge on this organelle has been totally lacking in molecular terms. In this study, we examined for the first time the occurrence and distribution of centriolar satellites/fibrous granules systemically in various mouse cells and tissues by immunofluorescence microscopy with anti-mPCM-1 pAb, and found that these granules were detected in all the types of mouse cells we examined. As these granules were not always concentrated around centrosomes, we tentatively called them ‘PCM-1 granules’ in this study. Although their abundance varied depending on the cell types, their localization could be explained by our previous observation that PCM-1 granules were transported along microtubules toward their minus ends (Kubo et al., 1999); for example, a large number of PCM-1 granules were enriched in the apical region of the cytoplasm of simple epithelial cells such as intestinal epithelial cells, where most of the minus ends of microtubules were located (Mogensen, 1999). Such widespread occurrence of PCM-1 granules and their intriguing distribution pattern urged us to examine their structure and functions further at the molecular level.

Yeast two-hybrid analyses revealed that PCM-1 molecules self-associate directly through their two distinct regions (aa 201-494 and aa 745-1128). Furthermore, when the PCM-1 fragments containing each or both of these regions was overexpressed, they formed large aggregates within the cytoplasm. These aggregates were similar to PCM-1 granules in their electron density at the electron microscopic level, and the isolated aggregates were mainly composed of PCM-1 with no major additional components. It remains unclear what molecules are contained in the in situ PCM-1 granules in addition to PCM-1 until they were isolated from cells to the homogeneity, but it is safe to say that PCM-1 constitutes the scaffolds of PCM-1 granules through its self-aggregation. Interestingly, detailed transfection experiments with various PCM-1 mutants suggested that the C-terminal region of PCM-1 molecules suppressed their self-aggregation. Thus, we were led to speculate that this C-terminal region is responsible for determining the size of individual PCM-1 granules.

The PCM-1 immunofluorescence signal was reported to disappear from the centrosomes when the cells entered the mitotic phase, although the expression level of PCM-1 appeared to be kept constant throughout the cell cycle (Balczon et al., 1994). Furthermore, previous electron

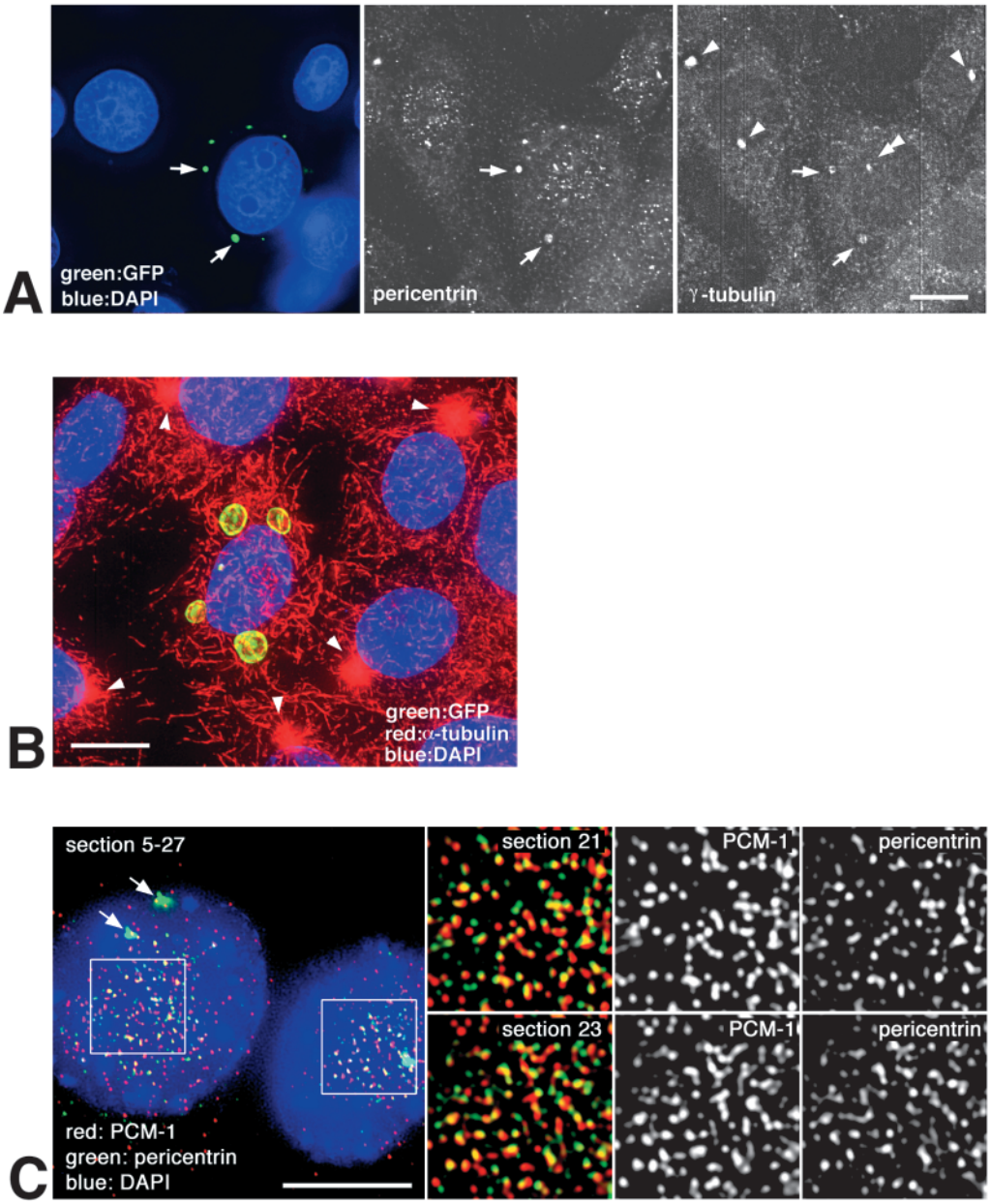

Fig. 5. PCM-1 granules and pericentrin. (A) A GFP fusion protein with a truncated XPCM-1 (aa 745-1128) was transiently overexpressed in A6 cells, in which several large aggregates were formed (arrows). Cells were fixed and double stained with rabbit anti-pericentrin pAb and mouse anti-γ-tubulin mAb, which were detected with rhodamine-conjugated anti-rabbit IgG antibody and Cy5-conjugated anti-mouse IgG antibody, respectively. Both endogenous pericentrin and γ-tubulin were recruited to the large aggregates of XPCM-1 mutant (arrows). In the absence of anti-pericentrin pAb or mouse anti-γ-tubulin mAb, pericentrin or γ-tubulin signals, respectively, disappeared from the large aggregates of XPCM-1 mutant, indicating that these signals were not artifacts caused by the GFP emission in additional wavelengths (data not shown). Notice that the amount of γ-tubulin at the centrosomes in the transfectants (double arrowheads) was significantly smaller than that in the surrounding parental cells (arrowheads). Bar, 10 μm. (B) A6 cells with or without the large aggregates of a GFP fusion protein with a truncated XPCM-1 (aa 745-1128) were incubated in a medium containing 0.4 μM nocodazole for 1 hour to depolymerize the microtubules, washed with fresh medium twice, incubated in fresh medium for 5 minutes to repolymerize the microtubules and then double stained with anti-α-tubulin mAb (red) and DAPI (blue). A large number of microtubules elongated from the centrosomes in A6 cells without large aggregates (arrowhead), whereas, in A6 cells bearing large aggregates, only a small number of microtubules were associated with the centrosomes. Bar, 10 μm. (C) Mouse CSG cells were triple stained with anti-mPCM-1 pAb (red), anti-mouse pericentrin mAb (green) and DAPI (blue), and observed by sectioning microscopy. Images were obtained at 0.2-μm intervals on the *z* axis and deconvolved with DeltaVision software. Left panels represent an integrated image of 23 sections. Most pericentrin was concentrated in the pericentriolar region (arrows), but the rest was scattered in the cytoplasm as granules. By contrast, most of the PCM-1 granules were distributed throughout the cytoplasm. The 21st section of the left boxed area and the 23rd section of the right boxed area (in the left panel) are enlarged in the right panels. Pericentrin granules (green) appeared to be scattered in the cytoplasm as distinct granules from PCM-1 granules (red), and these two types of granules were frequently associated with each other in a granule-to-granule manner (yellow). Bar, 10 μm.

microscopic observations demonstrated that centriolar satellites were not detected around the centrioles in dividing cells (Rattner, 1992). Therefore, taking our present observations together, we concluded that PCM-1 granules are disassembled at the mitotic phase. Interestingly, the large aggregates induced by mutant PCM-1 were also decreased in size during the mitotic phase. These findings suggested that, at the mitotic phase, the self-aggregation (i.e. the intermolecular association) of PCM-1 was suppressed within the cells to disassemble PCM-1 granules. The molecular mechanism of this suppression should be interesting; for example, the possible involvement of mitotic phase-specific phosphorylation of PCM-1 should be examined. Furthermore, the physiological relevance of the disassembly of PCM-1 granules should also be clarified. An interesting speculation is that at the mitotic phase PCM-1 or other unidentified

components of PCM-1 granules might be released into the cytoplasm in a soluble form, which might play some important role in mitotic-phase-specific events.

Some fractions of pericentrin were reported to exist in the cytoplasm as granular structures, although most fractions were concentrated in the pericentriolar region throughout cell cycle (Dictenberg et al., 1998; Young et al., 2000). Close inspection by immunofluorescence microscopy revealed that pericentrin granules were distributed in the cytoplasm as distinct structures from PCM-1 granules, and were frequently associated with PCM-1 granules in a granule-to-granule manner. Consistent with this finding, PCM-1 was reported biochemically to bind directly to pericentrin (Li et al., 2001). Pericentrin granules were reported to be associated with dynein and γ-tubulin, and to be transported along microtubules toward their minus ends to supply pericentrin and γ-tubulin to the centrosomes (Young et al., 2000; Zimmerman and Doxsey, 2000). PCM-1 granules were also shown to be transported along microtubules in the same direction (Kubo et al., 1999). Therefore, it is tempting to speculate that PCM-1 granules might function as cargo carrying some centrosomal components other than pericentrin/γ-tubulin, and that these two distinct types of granules interact mutually and dynamically on the way to the centrosomes. However, the information on the components of PCM-1 granules is still fragmentary and it is still premature to discuss further the physiological functions of PCM-1 granules.

As a continuation of our previous study, we have here further characterized PCM-1 granules (i.e. centriolar satellites/fibrous granules) in molecular terms. These data should be indispensable for future studies of the functions of PCM-1 granules, including the knockout of the PCM-1 gene.

We thank N. Shiina (National Institute of Genetics, Mishima, Japan) for his valuable discussions. This study was supported in part by a Grant-in-Aid for Cancer Research and a Grant-in-Aid for Scientific Research (A) from the Ministry of Education, Science and Culture of Japan.

References

Anderson, R. G. and Brenner, R. M. (1971). The formation of basal bodies (centrioles) in the Rhesus monkey oviduct. *J. Cell Biol.* **50**, 10-34.

Balczon, R. and West, K. (1991). The identification of mammalian centrosomal antigens using human autoimmune anticentrosome antisera. *Cell Motil. Cytoskeleton* **20**, 121-135.

Balczon, R., Bao, L. and Zimmer, W. E. (1994). PCM-1, A 228-kD centrosome autoantigen with a distinct cell cycle distribution. *J. Cell Biol.* **124**, 783-793.

Bernhard, W. and de Harven, E. (1960). L'ultrastructure du centriole et d'autres elements de l'appareil achromatique. In *Fourth International Conference on Electron Microscopy* (eds W. Bargmann, D. Peters and C. Wolpers), pp. 218-227. Berlin: Springer-Verlag.

Berns, M. W., Rattner, J. B., Brenner, S. and Meredith, S. (1977). The role of the centriolar region in animal cell mitosis. A laser microbeam study. *J. Cell Biol.* **72**, 351-367.

Bessis, M. and Breton-Gorius, J. (1958). Sur une structure inframicroscopique pericentriolaire. Etude au microscope electronique sur les leucocytes des mammiferes. *C. R. Acad. Sci.* **246**, 1289.

Bornens, M. and Moudjou, M. (1999). Studying the composition and function of centrosomes in vertebrates. *Methods Cell Biol.* **61**, 13-34.

de-Thé, G. (1964). Cytoplasmic microtubules in different animal cells. *J. Cell Biol.* **23**, 265-275.

Dictenberg, J. B., Zimmerman, W., Sparks, C. A., Young, A., Vidair, C., Zheng, Y., Carrington, W., Fay, F. S. and Doxsey, S. J. (1998). Pericentrin and γ-tubulin form a protein complex and are organized into a novel lattice at the centrosome. *J. Cell Biol.* **141**, 163-174.

Dirksen, E. R. (1991). Centriole and basal body formation during ciliogenesis revisited. *Biol. Cell* **72**, 31-38.

Kimble, M. and Kuriyama, R. (1992). Functional components of microtubule-organizing centers. *Int. Rev. Cytol.* **136**, 1-50.

Kubo, A., Sasaki, H., Yuba-Kubo, A., Tsukita, S. and Shiina, N. (1999). Centriolar satellites: molecular characterization, ATP-dependent movement toward centrioles and possible involvement in ciliogenesis. *J. Cell Biol.* **147**, 969-980.

Li, Q., Hansen, D., Killilea, A., Joshi, H. C., Palazzo, R. E. and Balczon, R. (2001). Kendrin/pericentrin-B, a centrosome protein with homology to pericentrin that complexes with PCM-1. *J. Cell Sci.* **114**, 797-809.

Lupas, A., van Dyke, M. and Stock, J. (1991). Predicting coiled coils from protein sequences. *Science* **252**, 1162-1164.

Mogensen, M. M. (1999). Microtubule release and capture in epithelial cells. *Biol. Cell* **91**, 331-341.

Osborn, T. G., Patel, N. J., Ross, S. C. and Bauer, N. E. (1982). Antinuclear antibody staining only centrioles in a patient with scleroderma. *New Engl. J. Med.* **307**, 253-254.

Rattner, J. B. (1992). Ultrastructure of centrosome domains and identification of their protein components. In *The Centrosome*, (ed. V. I. Kalnins), pp. 45-69. San Diego, CA: Academic Press.

Rattner, J. B., Mack, G. J. and Fritzler, M. J. (1998). Autoantibodies to components of the mitotic apparatus. *Mol. Biol. Rep.* **25**, 143-155.

Saitou, M., Ando-Akatsuka, Y., Itoh, M., Furuse, M., Inazawa, J., Fujimoto, K. and Tsukita, S. (1997). Mammalian occludin in epithelial cells: its expression and subcellular distribution. *Eur. J. Cell Biol.* **73**, 222-231.

Shiina, N., Moriguchi, T., Ohta, K., Gotoh, Y. and Nishida, E. (1992). Regulation of a major microtubule-associated protein by MPF and MAP kinase. *EMBO J.* **11**, 3977-3984.

Sorokin, S. P. (1968). Reconstructions of centriole formation and ciliogenesis in mammalian lungs. *J. Cell Sci.* **3**, 207-230.

Steinman, R. M. (1968). An electron microscopic study of ciliogenesis in developing epidermis and trachea in the embryo of *Xenopus laevis*. *Am. J. Anat.* **122**, 19-55.

Young, A., Dictenberg, J. B., Purohit, A., Tuft, R. and Doxsey, S. J. (2000). Cytoplasmic dynein-mediated assembly of pericentrin and γ-tubulin onto centrosomes. *Mol. Biol. Cell* **11**, 2047-2056.

Zimmerman, W. and Doxsey, S. J. (2000). Construction of centrosomes and spindle poles by molecular motor-driven assembly of protein particles. *Traffic* **1**, 927-934.